Sauer, R. T., & Anderegg, R. (1978) *Biochemistry 17*, 1092–1100.
Sauer, R. T., Pabo, C. O., Meyer, B. J., Ptashne, M., & Backman, K. C. (1979) *Nature (London) 279*, 396–400.
Sauer, R. T., Hehir, K., Stearman, R. S., Weiss, M. A., Jeitler-Nilsson, A., Suchanek, E. G., & Pabo, C. O. (1986) *Biochemistry 25*, 5992–5998.
Shih, H. H.-L., Brady, J., & Karplus, M. (1985) *Proc. Natl. Acad. Sci. U.S.A. 82*, 1697–1701.
States, D. J., Haberkorn, R. A., & Ruben, D. J. (1982) *J. Magn. Reson. 48*, 286–292.
States, D. J., Dobson, C. M., Karplus, M., & Creighton, T. E. (1984) *J. Mol. Biol. 174*, 411–418.
Wade-Jardetzky, N., Bray, R. P., Conover, W. W., Jardetzky, O., Geisler, N., & Weber, K. (1979) *J. Mol. Biol. 128*, 259–264.
Wagner, G., & Wüthrich, K. (1982) *J. Mol. Biol. 155*, 347–366.
Weber, K., & Geisler, N. (1978) in *The Operon* (Miller, J., & Reznikoff, W., Eds.) pp 155–163, Cold Spring Harbor Press, Cold Spring Harbor, NY.
Weber, P. L., Drobny, G., & Reid, B. R. (1985) *Biochemistry 24*, 4549–4552.
Weiss, M. A., Karplus, M., Patel, D. J., & Sauer, R. T. (1983) *J. Biomol. Struct. Dyn. 1*, 151–157.
Weiss, M. A., Sauer, R. T., Patel, D. J., & Karplus, M. (1984) *Biochemistry 23*, 5090–5095.
Weiss, M. A., Redfield, A. G., & Griffey, R. H. (1986) *Proc. Natl. Acad. Sci. U.S.A. 83*, 1325–1329.
Weiss, M. A., Pabo, C. O., Karplus, M., & Sauer, R. T. (1987) *Biochemistry* (following paper in this issue).
Wüthrich, K. (1976) *NMR in Biological Research: Peptides and Proteins*, Elsevier, New York.
Wüthrich, K., Wider, G., Wagner, G., & Braun, W. (1982) *J. Mol. Biol. 155*, 311–319.
Zuiderweg, E. R., Kaptein, R., & Wüthrich, K. (1983) *Proc. Natl. Acad. Sci. U.S.A. 80*, 5837–5841.

Dimerization of the Operator Binding Domain of Phage λ Repressor†

Michael A. Weiss,‡,§ Carl O. Pabo,‖ Martin Karplus,*,‡ and Robert T. Sauer⊥

Department of Chemistry, Harvard University, Cambridge, Massachusetts 02138, Department of Medicine, Brigham and Women's Hospital, Boston, Massachusetts 02115, Department of Biophysics, The Johns Hopkins School of Medicine, Baltimore, Maryland 21205, and Department of Biology, Massachusetts Institute of Technology, Cambridge, Massachusetts 02139

Received June 10, 1986; Revised Manuscript Received September 19, 1986

ABSTRACT: Dimerization of λ repressor is required for its binding to operator DNA. As part of a continuing study of the structural basis of the coupling between dimer formation and operator binding, we have undertaken ^{1}H NMR and gel filtration studies of the dimerization of the N-terminal domain of λ repressor. Five protein fragments have been studied: three are wild-type fragments of different length (1–102, 1–92, and 1–90), and two are fragments bearing single amino acid substitutions in residues involved in the dimer interface (1–102, Tyr-88 → Cys; 1–92, Ile-84 → Ser). The tertiary structure of each species is essentially the same, as monitored by the ^{1}H NMR resonances of internal aromatic groups. However, significant differences are observed in their dimerization properties. ^{1}H NMR resonances of aromatic residues that are involved in the dimer contact allow the monomer–dimer equilibrium to be monitored in solution. The structure of the wild-type dimer contact appears to be similar to that deduced from X-ray crystallography and involves the hydrophobic packing of symmetry-related helices (helix 5) from each monomer. Removal of two contact residues, Val-91 and Ser-92, by limited proteolysis disrupts this interaction and also prevents crystallization. The Ile-84 → Ser substitution also disrupts this interaction, which accounts for the severely reduced operator affinity of this mutant protein.

The λ repressor regulates gene expression by binding, as a dimer, to specific sequences of operator DNA (Chadwick et al., 1971; Johnson et al., 1980). Because dimer formation and DNA binding are coupled equilibria, dimerization contributes to apparent operator affinity. The intact repressor has not been crystallized, but studies of isolated proteolytic fragments suggest that there are two sets of dimer contacts; an N-terminal fragment (residues 1–92) crystallizes as a dimer (Pabo & Lewis, 1982), and a C-terminal fragment (residues 93–236) dimerizes readily in solution (Pabo et al., 1979). The N-terminal domain of repressor appears to mediate all of the contacts with operator DNA (Sauer et al., 1979), but it is likely that both N-terminal and C-terminal quaternary interactions contribute to the strength of operator binding. The importance of the C-terminal contacts has been inferred from the finding that intact repressor binds operator DNA at concentrations about 100-fold lower than those required to observe operator binding by N-terminal fragments. The importance of N-terminal dimerization has been inferred from the operator DNA protection patterns exhibited by N-terminal fragments (Sauer et al., 1979; Johnson, 1980), from consid-

† This work was supported in part by grants from the National Institutes of Health to M.K. (GM-37292), C.O.P. (GM-31471), and R.T.S. (AI-15706).
‡ Harvard University.
§ Brigham and Women's Hospital.
‖ The Johns Hopkins School of Medicine.
⊥ Massachusetts Institute of Technology.

0006-2960/87/0426-0897$01.50/0

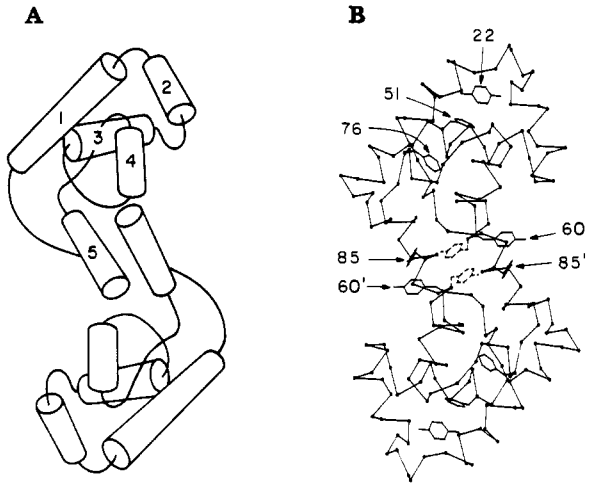

FIGURE 1: (A) Model of the 1–92 dimer. The α-helices are shown as cylinders. The first four helices form a globular domain, and the fifth extends outward as a dimer contact. (B) α-Carbon representation showing the aromatic side chains. Their ^{1}H NMR resonances provide sensitive markers for tertiary and quaternary structure. The structures shown are calculated from the crystal coordinates of Pabo and Lewis (1982).

erations of the relative DNA binding affinities of intact repressor and the N-terminal fragments (Pabo, 1980), and from model building of the protein–DNA complex with the crystal structure of the N-terminal dimer (Pabo & Lewis, 1982; Lewis et al., 1983).

The crystal structure of the dimer of the N-terminal fragment (residues 1–92) is shown in Figure 1 (Pabo & Lewis, 1982). As depicted in panel A, each monomer consists of five α-helices. The first four form a globular domain, and the fifth extends outward to pack against a symmetry-related helix 5 from another monomer. Helix 5 is amphipathic, and the dimer interaction is primarily hydrophobic. In the dimer, the DNA binding surfaces (helix 2–turn–helix 3) of each monomer are appropriately oriented to contact successive major grooves of B-DNA. To demonstrate that such a dimer forms in solution and to define its role in DNA binding, we have undertaken a biochemical and ^{1}H NMR study of wild-type and genetically altered N-terminal fragments. We show that the resonances of tyrosine side chains, which are involved in the crystallographic dimer contact, are perturbed as a function of concentration. Dimerization alters the local magnetic environments of residues in helix 5 but does not perturb the tertiary structure of the remainder of the domain. The helix 5–helix 5 interaction is shown to be disrupted by limited proteolysis or by mutations, and these effects are easily rationalized from the crystal structure (Pabo & Lewis, 1982). These data provide direct evidence that the N-terminal quaternary contacts are involved in maintaining the active operator binding conformation of the intact repressor dimer.

Materials and Methods

Protein Purification. The wild-type and Ile-84 → Ser repressor (Hecht et al., 1983) were purified from strains of *Escherichia coli* (W3110*lac*I^Q) containing plasmid pEA305 (Amann et al., 1983) by the method of Johnson et al. (1980). The wild-type and Tyr-88 → Cys mutant 1–102 fragments were purified from overproducing strains of *E. coli* as described (Weiss et al., 1984; Sauer et al., 1986).

Papain Fragments. Limited proteolysis of intact λ repressor with papain generates an N-terminal fragment containing residues 1–92 (Pabo et al., 1979). However, we have also observed formation of another N-terminal fragment whose

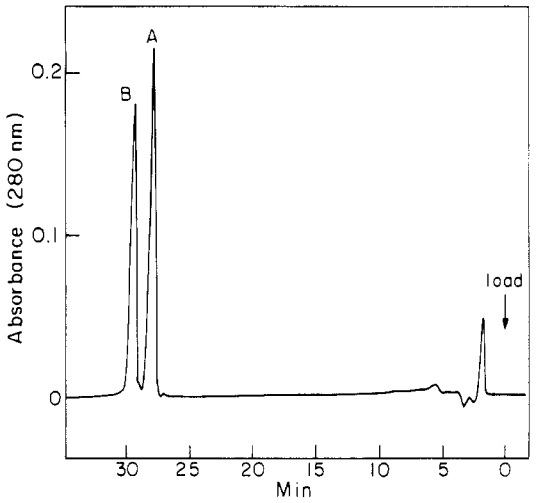

FIGURE 2: High-performance liquid chromatography (HPLC) separation of fragments 1–92 (peak a) and 1–90 (peak b) on a 10-μm C_{18} Z-module (Waters) column.

yield depends upon the conditions used for proteolysis. The 1–92 fragment is the major N-terminal species at early time points in the papain digestion; the other N-terminal fragment is the predominant product at longer reaction times. The two species can be separated by high-performance liquid chromatography (HPLC) or column chromatography with phenyl-Sepharose 4B. As we demonstrate below, the N-terminal fragment that appears late during the digestion corresponds to residues 1–90 of intact repressor.

The two N-terminal fragments were separated by HPLC with a 10-μm C_{18} Z-module (Waters) column, as shown in Figure 2. The protein was loaded in 0.1% trifluoroacetic acid (TFA) and eluted by an acetonitrile gradient ending with 60% acetonitrile and 0.04% TFA. Partial separation can also be obtained with a 200-mL phenyl-Sepharose 4B column equilibrated in buffer A (BA; see below) plus 3 M KCl. The protein solution (100 mg in 100 mL) was loaded in this buffer and eluted at a flow rate of 2–4 mL/min by a salt gradient from BA + 3 M KCl to BA + 0 M KCl; each reservoir contained 3 column volumes of buffer. The two N-terminal fragments elute as broad, incompletely resolved peaks: fragment 1–90 begins to elute near 1.5 M KCl and fragment 1–92 near 1 M KCl in the gradient. Nearly pure species may be obtained by pooling peak fractions and rerunning the column.

Analytical Gel Filtration. Small-zone gel filtration experiments were performed with the wild-type and Cys-88 mutant 1–102 fragments. Size standards of various molecular weights were used to calibrate the column as described in the legend to Table I. Experiments were conducted at room temperature in buffer B (see below).

Crystallization. Crystallization experiments with the N-terminal papain fragments were performed as described (Pabo, 1980; Pabo & Lewis, 1982).

NMR. For ^{1}H NMR study, the 1–102 fragment was exhaustively dialyzed against 50 mM ammonium bicarbonate, lyophilized, dissolved in D_2O, lyophilized, dissolved in 340 μL of NMR buffer (see below), and lyophilized. The powder was dissolved in 340 μL of 99.96% D_2O, spun for 1 min in a microcentrifuge, and loaded into a 5-mm NMR tube. The 1–92 and 1–90 fragments were exhaustively dialyzed against distilled, deionized water, lyophilized, dissolved in 340 μL or NMR buffer, and loaded into a 5-mm NMR tube.

All spectra were taken at 500 MHz with simultaneous quadrature-phase detection. One-dimensional free induction decays were acquired following a 70° pulse and processed as

Table I: Amino Composition of Wild-Type Repressor Fragments

	1–90		1–92		1–102	
	obsd	theory	obsd	theory	obsd	theory
Asx	7.03	7	6.79	7	6.90	7
Thr	1.83	2	1.65	2	1.56	2
Ser	6.35	7	6.56	8	8.85	9
Glx	13.89	14	13.86	14	17.10	17
Pro	1.90	2	2.15	2	2.75	3
Gly	5.93	6	5.78	6	5.85	6
Ala	10.51	11	10.56	11	10.61	11
Cys	ND[a]	0	ND	0	ND	0
Val	4.20	4	5.02	5	4.96	5
Met	2.80	3	2.81	3	3.93	4
Ile	4.71	5	4.61	5	4.70	5
Leu	10.23	10	10.10	10	11.31	11
Tyr	3.43	4	3.61	4	4.55	5
Phe	2.06	2	2.01	2	2.06	2
His	0.00	0	0.03	0	0.06	0
Lys	9.88	10	9.79	10	9.99	10
Arg	2.98	3	2.89	3	4.15	4
Trp	ND	0	ND	0	ND	0

[a] ND = not determined.

Table II: Amino Acids Released by Carboxypeptidase Digestion

fragment	C-terminal residues
1–90	Ala, Glu
1–92	Ser, Val
1–92, Ile 84 → Ser	Ser, Val
1–102	Glu, Tyr

described in the legends to Figures 3–6. Two-dimensional correlated and Overhauser spectra were obtained by the pure-phase method of States and co-workers (Aue et al., 1976; States et al., 1982).

Protein Chemistry. Amino acid compositions were obtained following acid hydrolysis. N-Terminal Edman degradation was performed by standard methods (Sauer & Anderegg, 1978). C-Terminal residues were identified following digestion with carboxypeptidase A (Sigma). The amino acid sequence of the Ile-84 → Ser mutant repressor was inferred by DNA sequencing (Hecht et al., 1983) and confirmed by determining the amino acid composition of a difference tryptic peptide (data not shown).

Buffers. Buffer A consists of 5% glycerol, 10 mM tris(hydroxymethyl)aminomethane hydrochloride (Tris-HCl) (pH 8.0), 1.4 mM β-mercaptoethanol, 0.1 mM ethylenediaminetetraacetic acid (EDTA), and 0.1 mM sodium azide. Buffer B consists of 50 mM Tris-HCl (pH 7.5), 200 mM NaCl, and 1 mM EDTA. NMR buffer consists of 200 mM KCl, 50 mM potassium phosphate (pD 7.4, direct meter reading), 1 mM sodium azide, and 0.1 mM EDTA.

Results

N-Terminal repressor fragments of different lengths can be generated by limited proteolysis of intact protein or by recombinant DNA techniques involving deletion of C-terminal sequences. In this paper we study three such fragments, consisting of residues 1–90, 1–92, and 1–102, that were prepared as described under Materials and Methods. Their identities are confirmed by their respective amino acid compositions and the residues released by carboxypeptidase digestion (Tables I and II). Each of the fragments has the same N-terminal sequence (Ser-Thr-Lys-Lys-Lys) as intact λ repressor.

Gel Filtration. Oligomerization of the 1–92 N-terminal fragment of λ repressor was originally investigated by equilibrium ultracentrifugation (Pabo et al., 1979). It was found to be predominantly monomeric at a concentration of 50 μM.

Table III: Small-Zone Gel Filtration

species	loading concn (M)	σ
standards		
thyroglobulin (670 kDa)		0.000
ovalbumin (45 kDa)		0.162
myoglobin (17 kDa)		0.437
aprotinin (6.5 kDa)		0.700
vitamin B12 (1.3 kDa)		1.000
wild-type 1–102 fragment	3.3×10^{-6}	0.466
	2.5×10^{-5}	0.440
	1.0×10^{-4}	0.427
	4.5×10^{-4}	0.376
Tyr-88 → Cys covalent dimer	3.2×10^{-6}	0.298
	3.1×10^{-5}	0.294

Table IV: Summary of Aromatic Assignments (1–92 and 1–102 Dimer)

peak[a]	residue
a	Phe-76 para
b	Tyr-85 ortho
c	Tyr-60 ortho
d	Tyr-101 ortho
e	Phe-76 meta
f	Phe-76 ortho, Tyr-60 meta
g	Phe-51 ortho, Tyr-85 meta, Tyr-101 meta[b]
h	Tyr-22 ortho
i	Tyr-88 meta, Tyr-22 meta
j	Phe-51 meta
k	Phe-51 para

[a] As shown in Figure 3. [b] Not observed in 1–92 spectrum.

We have used small-zone gel filtration to study the chromatographic properties of the 1–102 fragment as a function of loading concentration in the range 3–450 μM. The data are shown in Table III. At low concentrations, the fragment runs at a position near that expected for a monomer. At the highest concentration tested, however, the fragment eluted at a position about halfway between that expected for a monomer and that expected for a dimer. Although these data cannot be interpreted quantitatively (Ackers, 1970), they suggest that the 1–102 fragment is undergoing a monomer–dimer transition in this concentration range.

Concentration Dependence of ^1H NMR Spectrum. An NMR study of the 1–102 fragment at high concentration (5 mM) demonstrates that the major features of the crystallographic dimer are retained in solution [see the preceding paper (Weiss et al., 1987)]. The resonances of Tyr-88 are shifted upfield, as expected from its stacking interaction with Tyr-88′, and a nuclear Overhauser effect (NOE) is observed between Tyr-88 and Tyr-85′, as predicted from the crystallographic dimer. The positions of the aromatic side chains in the crystal structure are shown in Figure 1, and their ^1H NMR assignments are summarized in Table IV and Figure 3.

The ^1H NMR spectrum of the 1–102 fragment at a series of concentrations is shown in Figure 3. In the bottom spectrum, the protein concentration is 75 μM; in the top spectrum, the protein concentration is 3.6 mM. The resonances of Tyr-22 and Phe-51 (which are buried residues) are nearly independent of concentration, indicating that the tertiary structure of the N-terminal domain is not perturbed by dimerization. Significant changes are observed in the resonances of Tyr-85 and Tyr-88, whose environments are influenced by quaternary interactions in the crystal structure (Pabo & Lewis, 1982). The meta resonance of Tyr-88 in the dimer (peak i in Figure 3, which also contains the meta resonance of Tyr-22) decreases in amplitude with decreasing concentration. Because its amplitude rather than its chemical shift changes with protein concentration, it appears to be in slow exchange between

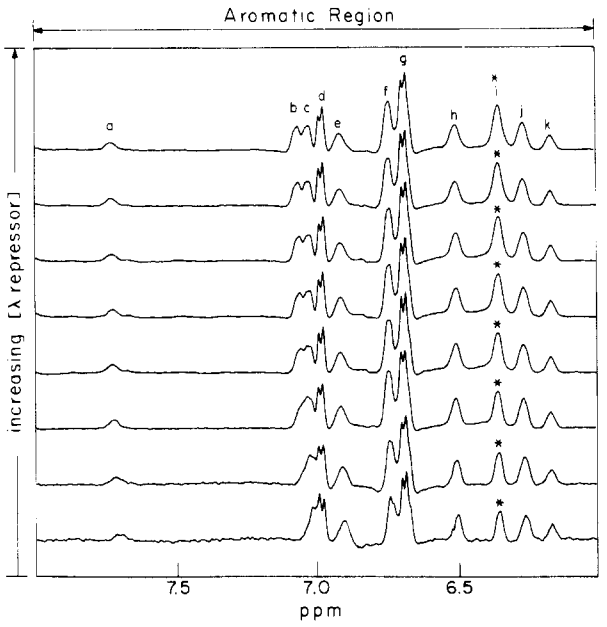

FIGURE 3: Aromatic ^{1}H NMR spectra of the 1–102 domain at a series of concentrations at 30 °C. In the bottom spectrum, the protein concentration is 75 μM. Successive concentrations are 150 μM, 300 μM, 600 μM, 900 μM, 1.2 mM, 2.1 mM, and 3.6 mM (top spectrum). No further spectroscopic changes are observed at concentrations greater than 3.6 mM. The meta resonance of Tyr-88 overlaps that of Tyr-22 and is indicated by an asterisk. The assignments of peaks a–k in the top spectrum are given in Table IV. The 75 μM spectrum is the sum of 6000 scans; successive spectra are the sum of 3836, 3416, 1124, 500, 356, 176, and 100 scans, respectively. The recycle delay was 2–4 s. Resolution was enhanced by convolution difference with parameters GM4, EM20, and 1.0. The base line was corrected with a spline function. Chemical shifts are relative to dioxane at 3.64 ppm. Amide protons were preexchanged in D_2O solution for 48 h at 30 °C.

monomer and dimer environments; the positions of the Tyr-88 resonances in the monomer have not been determined. The ortho resonance of Tyr-85 (peak b) shifts toward the random-coil frequency of Tyr-101 (peak d) with decreasing concentration. Shifts are also observed in the ortho resonance of Tyr-60 (0.05 ppm) and in the para resonance of Phe-76 (0.04 ppm). Because their frequencies rather than amplitudes change with concentration, Tyr-85, Tyr-60, and Phe-76 appear to be in fast exchange between monomer and dimer environments. These data are fit by a dimerization constant (K_d) of 0.3 mM (Feeney et al., 1979). Increases in the line width of ^{1}H NMR resonances without further changes in chemical shift or amplitude are observed when the protein concentration is raised from 3.5 to 7.0 mM (data not shown). This implies that higher order oligomerization is taking place at such high protein concentrations; these interactions apparently do not involve aromatic residues. The ^{1}H NMR transition observed at lower concentrations is consistent with a second-order reaction.

The ^{1}H NMR spectra of the 1–102 and 1–92 fragments are compared in Figure 4. Both species are dimeric at the concentrations and conditions used. The 1–92 fragment spectrum (panel B) is similar to that of the 1–102 fragment (panel A); the resonances of Tyr-22, Phe-51, and Phe-76 are not significantly shifted, indicating that the tertiary structure is not affected by residues 93–102. The Tyr-101 spin system (indicated by arrows in panel A) is absent in the 1–92 fragment spectrum, consistent with its amino acid composition. Small differences are observed in the chemical shifts of Tyr-60 and Tyr-85 in the two species (<0.05 ppm). This perturbation may reflect either structural, electrostatic, or diamagnetic effects of residues 93–102. The meta resonance of Tyr-88 has vir-

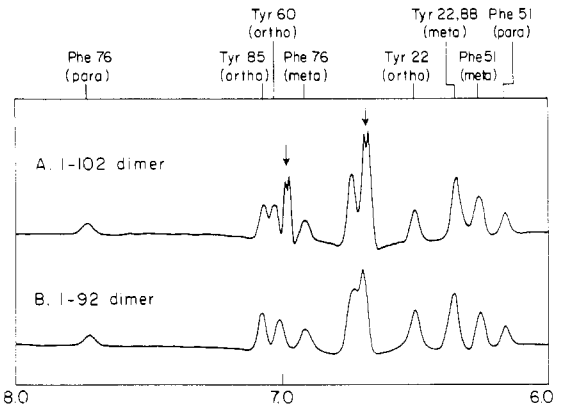

FIGURE 4: Aromatic ^{1}H NMR spectra of the 1–102 fragment (panel A) and the 1–92 fragment (panel B) at 5 mM concentration. The resonances of Tyr-101 are indicated by arrows. The fragments are dimeric at the concentrations and conditions used; the correspondence of their aromatic spectra indicates that their tertiary and quaternary structures are similar, with differences as described in text. Spectrum A is the sum of 100 transients with a recycle delay of 4 s. Spectrum B is the sum of 252 transients with a recycle delay of 2 s. The residual HOD signal was presaturated for 1 s. Resolution was enhanced by convolution difference with parameters GM4, EM20, and 1.0.

tually the same chemical shift in both species. In addition, the broad resonance near 6.5 ppm in the 1–92 fragment spectrum is more intense than in the 1–102 fragment spectrum (indicated by an asterisk in panel B of Figure 4). The additional intensity in the 1–92 fragment spectrum is assigned to the ortho protons of Tyr-88, the only protons unaccounted for in the spectrum. This is consistent with the assignment of the Tyr-88 ortho resonance in a mutant repressor, Tyr-85 → Cys, in which Tyr-88 is in fast exchange (Weiss et al., 1986). Presumably, the corresponding resonance in the wild-type 1–102 fragment spectrum is further broadened by intermediate exchange (ring rotation) and so is not seen. The dynamic implications of this difference are described below.

The ^{1}H NMR spectrum of the 1–92 fragment at a series of concentrations is shown in Figure 5. In the bottom spectrum, the protein concentration is 30 μM; in the top spectrum, it is 5.4 mM. Concentration-dependent perturbations are also observed for this species. As above, the resonances of Tyr-22, Phe-51, and Phe-76 are not significantly affected, indicating that the tertiary structure of the domain is not perturbed by dimerization. The broad resonances of Tyr-88 in the upfield region shift progressively downfield (i.e., toward random-coil frequencies) with decreasing concentration; they appear to be in fast to intermediate exchange between monomer and dimer environments. Likewise, the ortho resonances of Tyr-60 and Tyr-85 (peaks b and c) shift to the same frequency near 7 ppm with decreasing concentration; they are in fast exchange between dimer and monomer environments. As was observed for the 1–102 fragment, a small shift (0.04 ppm) is also observed in the para resonance of Phe-76 (peak a). The dimerization of the 1–92 fragment (K_d = 0.6 mM) is 2-fold weaker than that of the 1–102 fragment.

As the concentration of protein is decreased, the meta resonance of Tyr-88 in the dimer state shifts (in the case of fragment 1–92) or diminishes in amplitude (in the case of fragment 1–102). However, at the lowest concentration observed (30 μM) new resonances associated with Tyr-88 in the monomer state do not appear. Integration of the spectrum reveals that nearly four proton resonances are absent; these must be the ortho and meta resonances of Tyr-88, since all the other aromatic groups are accounted for in the spectrum. This implies that Tyr-88 is in intermediate exchange in the

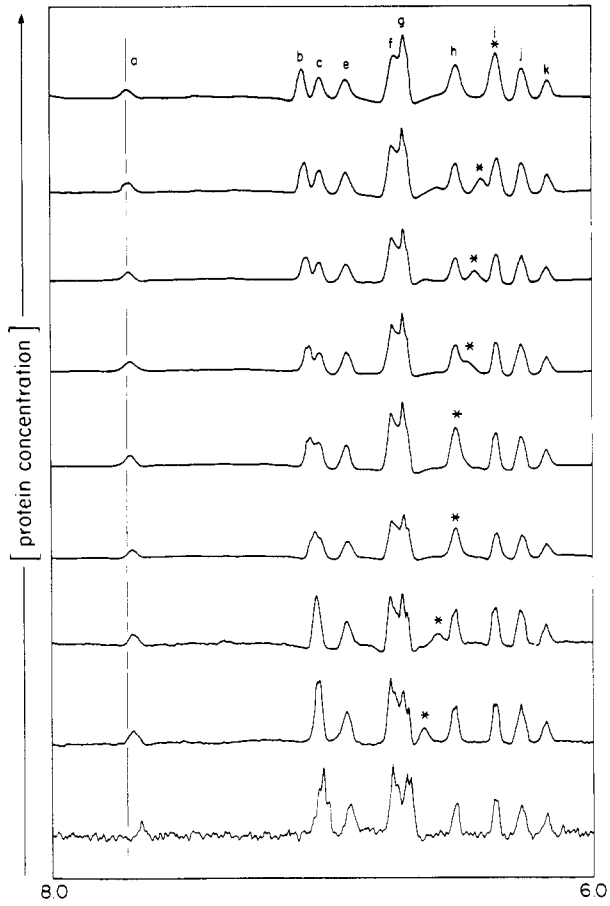

FIGURE 5: Aromatic spectrum of the 1–92 fragment at a series of concentrations. The meta resonance of Tyr-88 is indicated by an asterisk. The assignments of peaks a–k are given in Table IV. Small shifts are observed in the para resonance of Phe-76 (solid line). In the bottom spectrum, the protein concentration is 30 μM; successive concentrations are 150 μM, 300 μM, 600 μM, 900 μM, 1.2 mM, 1.8 mM, 2.7 mM, and 5 mM (top spectrum). The 30 μM spectrum is the sum of 22 256 scans; successive spectra are the sum of 5768, 3700, 2400, 1800, 1000, 224, 224, 232, and 252 scans, respectively. The recycle delay was 1.0–2.0 s. Conditions are as described in the legend to Figure 3.

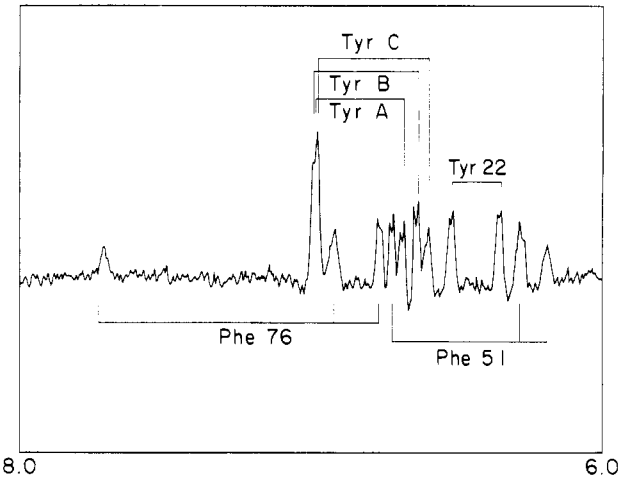

FIGURE 6: Aromatic spectrum of the 1–92 fragment at 1 mM concentration and pD 10.0. As demonstrated by the COSY spectrum (Figure 7), all four tyrosines (including Tyr-88) are observed under these conditions. These are labeled Tyr-22, Tyr-A, Tyr-B, and Tyr-C in the figure. The resonances of Phe-51 and Phe-76 are also indicated and are similar to their frequencies at pD 7.4. The pD was adjusted with NMR buffer + 100 mM D_2O. A convolution difference with parameters GM4, EM10, and 1.0 was applied.

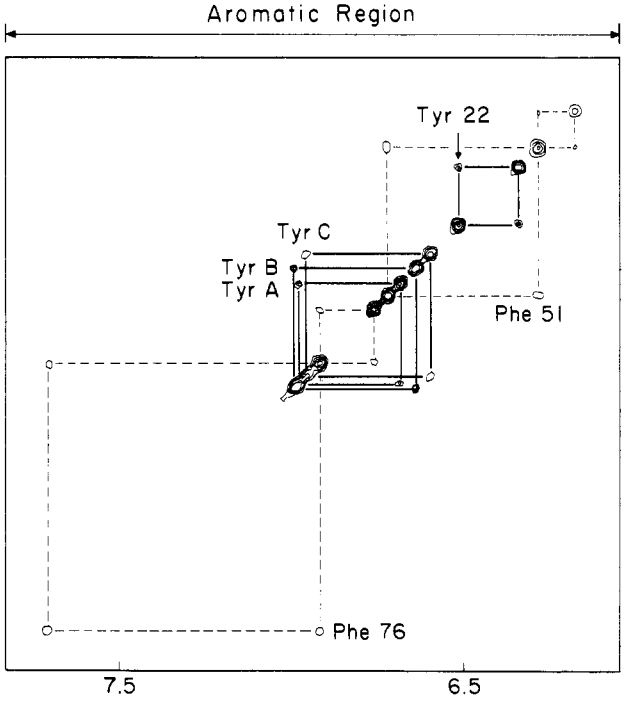

FIGURE 7: Two-dimensional phase-sensitive COSY spectrum of the 1–92 domain at pD 10.0. Four tyrosine spin systems (Tyr-22, Tyr-A, Tyr-B, and Tyr-C) are observed and are shown as solid lines. The two phenylalanine spin systems (Phe-51 and Phe-76) are shown as dashed lines. Although Tyr-88 has not been assigned, it is in fast exchange under these conditions. The COSY spectrum was recorded at 30 °C. A total of 1024 points were sampled over t_2 with a recycle delay of 1 s. Ninety-six scans were acquired per t_1 value, and 220 t_1 values were obtained. The t_1 dimension was zero-filled to create a square data matrix. A convolution difference with parameters GM3, EM20, and 1.0 was applied in both dimensions. The final data matrix was made symmetrical by minimum value.

monomer state. It is likely that residues 79–92 (the helix 5 region) participate in an intramolecular interaction in the monomer structure, although whether it remains as a helix has not been determined. The missing resonances may be recovered by raising the pH. The spectrum of the 1–92 fragment at 1 mM concentration at pH 10.0 is shown in Figure 6. There is no missing amplitude, and all four tyrosine spin systems are observed to be in fast exchange. These spin systems are shown in the correlated spectroscopy (COSY) spectrum in Figure 7. The tertiary structure of the domain is not perturbed at this pH, as indicated by the resonances of Tyr-22, Phe-51, and Phe-76. Presumably, partial ionization of the tyrosines destabilizes whatever structure is responsible for the constrained rotation of Tyr-88 in the monomer state.

The fast- and slow-exchange conditions allow upper and lower bounds for the lifetime τ_d of the 1–102 dimer to be estimated:

$$1/\Delta\nu_{slow} < \tau_d < 1/\Delta\nu_{fast}$$

where $\Delta\nu_{slow}$ is the difference in frequency between monomer and dimer states of a resonance related by slow exchange and $\Delta\nu_{fast}$ is the corresponding difference in fast exchange. If the resonances of Tyr-88 are assumed to be near those of the Tyr-60, Tyr-85, and Tyr-101 in the monomer state (i.e., near random-coil frequencies), then for the 1–102 fragment, the limits are 5 ms $< \tau_d <$ 50 ms. Thus, we may estimate the dissociation rate constant (k_d) to be (0.2–2) $\times 10^2$ s^{-1} and the association rate constant (k_a) to be approximately 10^6 s^{-1} M^{-1}. For the 1–92 dimer only an upper bound of 5 ms may be estimated, since no resonances are observed to be in slow exchange. Thus, the presence of residues 93–102 decreases

Table V: Dissociation and Rate Constants

fragment	K_d (M)	τ (s)	k_d (s^{-1})	k_a (s^{-1} M^{-1})
1–90	$>1 \times 10^{-1}$			
1–92	6×10^{-4}	$<10^{-2}$	$>10^2$	
1–92, Ile-84 → Ser	$>2 \times 10^{-2}$			
1–102	3×10^{-4}	10^{-2}	10^2	10^6

the dissociation rate; since the 1–92 and 1–102 fragment equilibrium dimerization constants are only 2-fold different, it is possible that the association rate is also affected. The inferred equilibrium and rate constants are summarized in Table V.

Tyr-88 Ring Dynamics. As indicated above, Tyr-88 has different exchange characteristics in the 1–92 and 1–102 dimers. In each fragment the meta protons are in fast exchange and the ortho protons in intermediate exchange. However, the extent of broadening of the ortho resonance is greater in the 1–102 dimer. This difference in exchange character implies that either (a) the Tyr-88 ring is rotating more rapidly in the smaller fragment, (b) the lifetime of its rotation state is limited by the lifetime of the dimer, or (c) the magnetic inequivalence between ortho sites is reduced in the smaller fragment. The latter mechanism is unlikely, since the chemical shifts of the Tyr-88 meta resonances are almost identical in the two species. The second mechanism is plausible. If Tyr-88 is in fast exchange in the monomer state, then the individual labels of its ortho protons in the dimer state become scrambled. In equilibrium, the lifetime of a label cannot exceed the lifetime of the dimer. The reduced lifetime of the 1–92 dimer is consistent with this mechanism. Alternatively, the change in exchange character of Tyr-88 in the 1–92 fragment may reflect a change in the local dynamics of the dimer state, reducing barriers to ring rotation (Karplus & McCammon, 1983). This mechanism is observed in the Tyr-85 → Cys mutant repressor (Weiss et al., 1987) and in a refolding intermediate of bovine pancreatic trypsin inhibitor (States et al., 1984). Both mechanisms may apply here and reflect the same types of molecular events that permit ring rotation or dissociation of the dimer (i.e., local packing defects).

Tyr-88 → Cys Mutant Domain. A mutant 1–102 repressor fragment has been described that contains an intermolecular disulfide bond (Sauer et al., 1986; Weiss et al., 1986). The mutation Tyr-88 → Cys was introduced by site-directed mutagenesis following predictions that such a bond could be accommodated within the native structure (Pabo & Suchanek, 1986). The resulting covalent dimer exhibits increased operator affinity.

As a control for the concentration-dependent effects observed for the wild-type 1–92 and 1–102 fragments, we have studied the Tyr-88 → Cys mutant 1–102 fragment at a series of concentrations. Because a covalent dimer cannot undergo a monomer–dimer transition, its ^{1}H NMR spectra should not be perturbed by protein concentration. In gel-filtration studies, the mutant fragment elutes at a position expected for a dimer, as indicated in Table III. No significant differences were observed between loading concentrations of 3.2 and 31 μM. Similarly, the ^{1}H NMR spectrum is not affected by protein concentration, as shown in Figure 8. In contrast to the wild-type spectra above, no changes in resonance amplitude or frequency are observed in the concentration range 0.5–5 mM. The assignment and structural implications of the mutant spectrum are described elsewhere (Weiss et al., 1987; Sauer et al., 1986).

Reducing N-Terminal Dimerization by Partial Proteolysis. The properties of the 1–90 fragment and of a mutant 1–92 fragment provide further information about dimerization. The

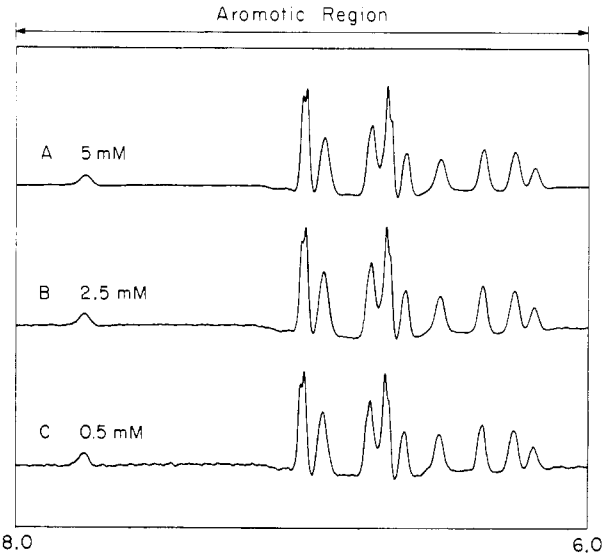

FIGURE 8: No concentration-dependent changes are observed in the spectrum of the Tyr-88 → Cys mutant 1–102 fragment, which forms a covalent dimer (Sauer et al., 1986). Spectrum A (5 mM protein concentration) is the sum of 1016 transients following a recycle delay of 2 s, during which the residual HOD solvent resonance was presaturated. Spectrum B (2.5 mM) is the sum of 1020 transients with a recycle delay of 2 s, and spectrum C (0.5 mM) is the sum of 1265 transients with a recycle delay of 1.5 s. Resolution was enhanced by convolution difference with parameters GM4, EM20, and 1.0.

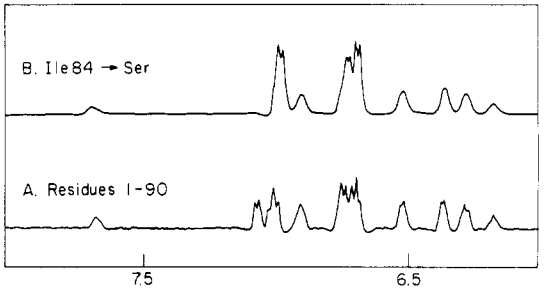

FIGURE 9: Dimerization of the 1–92 fragment is weakened by removal of residues 91 and 92 by partial proteolysis and by the mutation Ile-84 → Ser. (A) Aromatic ^{1}H NMR spectrum of the 1–90 papain fragment at 37 °C. The aromatic interactions in the helix 5 dimer contact are not observed. The protein concentration was 300 μM. The spectrum is the sum of 10 000 scans with a recycle delay of 1 s. No changes are observed in the concentration range 0.15–20 mM (data not shown). A convolution difference with parameters GM4, EM10, and 1.0 was applied. (B) Aromatic ^{1}H NMR spectrum of the Ile-84 → Ser 1–92 fragment at 30 °C. The protein concentration was 3 mM. No changes are observed in the concentration range 0.3–3 mM (data not shown). A convolution difference with parameters GM2, EM50, and 1.0 was applied.

aromatic region of the ^{1}H NMR spectrum of the 1–90 fragment is shown in panel A of Figure 9. The resonances of Tyr-22, Phe-51, and Phe-76 are not significantly perturbed, indicating that removal of Val-91 and Ser-92 does not disrupt the tertiary structure of the domain. In contrast to the longer fragments (1–92 or 1–102), no concentration-dependent shifts are observed in its NMR spectrum between 0.3 and 20 mM (data not shown). Two-dimensional correlated (COSY) and Overhauser (NOESY) spectra reveal three tyrosine spin systems (Tyr-60, Tyr-85, and Tyr-88) whose chemical shifts are near those of random-coil tyrosine (data not shown). Their respective ortho and meta resonances are equivalent, indicating fast exchange with respect to ring rotation. Although these spin systems are not individually assigned, it follows that the resonances of Tyr-88 do not exhibit the unusual shifts or constrained rotation observed in the 1–92 and 1–102 dimers.

In addition, no inter-tyrosine NOEs are observed. These changes indicate that the Tyr-88–Tyr-88′ and Tyr-88–Tyr-85′ interactions have been disrupted. Thus, the 1–90 fragment appears to be a monomer at the concentrations and conditions studied; if we assume that 20% dimer would have been detected, then $K_d > 128$ mM.

The impaired dimerization of fragment 1–90 may be rationalized from the crystal structure. In the crystal, Val-91 and Ser-92 participate in quaternary interactions. The side chain of Val-91 is packed in the hydrophobic interface between helix 5 and helix 5′, and Ser-92 appears properly positioned to contribute a hydrogen bond to Glu-74′. Removal of these residues would therefore be expected to destabilize the dimer. Further destabilization might arise through length-dependent or sequence-dependent reductions in the stability of helix 5.

The 1–90 fragment does not form crystals under conditions that resulted in crystallization of the 1–92 fragment (Pabo & Lewis, 1982). In addition, crystals grown from mixtures of fragments 1–90 and 1–92 contain only the longer fragment (data not shown). Since the dimer is a fundamental part of the crystallographic unit cell, the helix 5–helix 5 interaction apparently contributes to the stability of the crystal. This interaction is weakened for the 1–90 fragment, preventing its incorporation into the nascent crystal.

Reducing N-Terminal Dimerization by Mutation. The aromatic spectrum of a variant 1–92 fragment containing the mutation Ile-84 → Ser is shown in panel B of Figure 9. Its NMR properties are similar to those of fragment 1–90 above. Its tertiary structure is identical with that of wild-type, as indicated by the resonances of Tyr-22, Phe-51, and Phe-76. Three tyrosine spin systems (Tyr-60, Tyr-85, and Tyr-88) are observed in the NOESY and COSY spectra whose frequencies are near those of random-coil tyrosine. No inter-tyrosine NOEs are seen. No concentration-dependent shifts are observed between 0.3 and 3 mM. Thus, the Ile-84 → Ser 1–92 fragment dimerizes less readily ($K_d > 19$ mM, assuming that 20% dimer would have been detected) than wild-type fragment 1–92 ($K_d = 0.6$ mM). Its reduced dimerization may also be rationalized from the crystal structure. The substitution Ile-84 → Ser replaces a large hydrophobic residue in the subunit interface with a smaller hydrophilic side chain. As illustrated in Figure 10, Ile-84 packs against Met-87′, and also Val-91′. Presumably, the serine side chain in the mutant protein disrupts this hydrophobic interaction between helix 5 and helix 5′. Because the globular domain is unperturbed by the mutation, the DNA binding (helix 2–turn–helix 3) surface is intact. Thus, the impaired dimerization of this mutant must be reponsible for its loss of operator affinity, which is reduced at least 100-fold (Hecht et al., 1983; Nelson et al., 1983).

Discussion

We have shown that the N-terminal domain of λ repressor forms a dimer in solution, which is similar to that observed in the crystal. Because the dimer interface involves tyrosine ring interactions, the monomer–dimer transition may be monitored by ^{1}H NMR. Laser Raman studies described elsewhere (Thomas et al., 1986) demonstrate that tyrosine vibrational modes are also perturbed by dimerization.

In the dimer, Tyr-88 is stacked against Tyr-88′. These two rings are symmetry-related and therefore give rise to one set of resonances, which are shifted upfield in the dimer. Tyr-60 and Tyr-85, which are on the surface of the dimer, exhibit smaller downfield shifts. Small perturbations are also observed in the para resonance of Phe-76, which is in the turn between helix 4 and helix 5. These concentration-dependent effects are not observed in the spectrum of the 1–90 fragment. Since

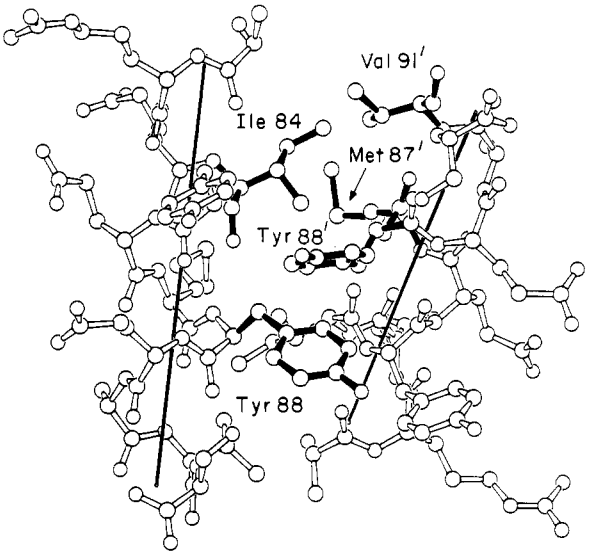

FIGURE 10: Ball-and-stick model of the helix 5–helix 5′ dimer contact. The side chains of Ile-84, Met-87′, and Val-91′ are indicated. Ile-84 is buried in the hydrophobic interface between dimer helices (helix 5). It packs against Met-87′ and Val-91′ from the other protomer. The mutation Ile-84 → Ser weakens dimerization at least 30-fold, presumably by disrupting this hydrophobic interaction. The helical axes are shown as solid lines; for clarity, the molecule has been slightly rotated from the projection shown in Figure 1. The structure shown is calculated from the crystal coordinates of Pabo and Lewis (1982).

no dimerization was detected, its equilibrium dissociation constant is weakened at least 200-fold relative to that of the 1–92 fragment. Similarly, the dissociation constant of a variant 1–92 fragment containing the mutation Ile-84 → Ser is weakened at least 30-fold. These results indicate that Ile-84, Val-91, and Ser-92 residues contribute to the stability of the dimer, as expected from the crystal structure.

The λ repressor recognizes operator DNA as a dimer (Chadwick et al., 1971). Because dimerization and DNA binding are coupled equilibria, this quaternary interaction contributes to apparent operator affinity. The λ operator site is almost symmetric (Maniatis et al., 1975), and the two repressor subunits are thought to make equivalent contacts with the two halves of the operator site (Pabo & Lewis, 1982). Thus, a longer DNA site is recognized, enhancing overall sequence specificity.

Both the C-terminal and N-terminal domains contain dimer contacts. The likely importance of N-terminal dimerization was initially inferred from its operator binding properties (Sauer et al., 1979; Pabo, 1980). Unlike monomeric fragments of *lac* repressor, which bind to half operator sites (Ogata & Gilbert, 1978), N-terminal fragments of λ repressor are observed to protect the entire operator in chemical probe experiments (Sauer et al., 1979; Johnson, 1980). This suggested that the N-terminal fragment binds cooperatively (as a dimer) to the full operator site. The apparent affinity of the N-terminal fragment for operator was also observed to be stronger than that expected for monomer binding. The dimer interaction subsequently observed in the crystal provided a structural basis for these effects.

Structural studies of the Ile-84 → Ser mutant provide direct evidence for the importance of N-terminal dimerization in DNA binding. This amino acid substitution does not perturb the DNA binding surface of each subunit;nevertheless, its operator affinity is reduced at least 100-fold (Hecht et al., 1983; Nelson et al., 1983). The reduction in DNA binding must be due to an altered N-terminal quaternary structure.

ACKNOWLEDGMENTS

We thank Mitch Lewis for helpful discussion; Anna Jeitler-Nilsson, Kathy Hehir, and Andrea Jeffrey for help with protein purification; Kathy Hehir and Andrea Jeffrey for protein sequencing; Michael Hecht, Robert Stearman, and Hillary Nelson for mutant plasmids; Eric Suchanek for computer graphics; Dinshaw Patel, David States, Jeff Hoch, David Ruben, Ponzy Lu, and Alfred Redfield for advice regarding NMR techniques; and Anne Lawthers for preparation of the manuscript. The 500-MHz spectra were recorded at the High-Field NMR Resource of the Francis Bitter National Magnet Laboratory (NIH, RR-00995).

REFERENCES

Ackers, G. K. (1970) *Adv. Protein Chem. 24*, 343–446.
Amann, E., Brosius, J., & Ptashne, M. (1983) *Gene 25*, 167–174.
Aue, W. P., Bartholdi, E., & Ernst, R. R. (1976) *J. Chem. Phys. 64*, 2229–2241.
Chadwick, P., Pirrotta, V., Steinberg, R., Hopkins, N., & Ptashne, M. (1971) *Cold Spring Harbor Symp. Quant. Biol. 35*, 283–294.
Feeney, J., Batchelor, J. G., Albrand, J. P., & Roberts, G. C. K. (1979) *J. Magn. Reson. 33*, 519–529.
Hecht, M. H., Nelson, H. C. M., & Sauer, R. T. (1983) *Proc. Natl. Acad. Sci. U.S.A. 80*, 2676–2680.
Johnson, A. D. (1980) Ph.D. Thesis, Harvard University.
Johnson, A. D., Pabo, C. O., & Sauer, R. T. (1980) *Methods Enzymol. 65*, 839–856.
Karplus, M., & McCammon, A. (1983) *Annu. Rev. Biochem. 52*, 263–300.
Lewis, M., Jeffrey, A., Wang, J., Ladner, R., Ptashne, M., & Pabo, C. O. (1983) *Cold Spring Harbor Symp. Quant. Biol. 47*, 435–440.
Maniatis, T., Ptashne, M., Backman, K., Kleid, D., Flashman, S., Jeffrey, A., & Mauer, R. (1975) *Cell (Cambridge, Mass.) 5*, 109–113.
Nelson, H. C. M., Hecht, M. H., & Sauer, R. T. (1983) *Cold Spring Harbor Symp. Quant. Biol. 47*, 441–449.
Ogata, R. T., & Gilbert, W. (1978) *Proc. Natl. Acad. Sci. U.S.A. 75*, 5851–5854.
Pabo, C. O. (1980) Ph.D. Thesis, Harvard University.
Pabo, C. O., & Lewis, M. (1982) *Nature (London) 298*, 443–447.
Pabo, C. O., & Suchanek, E. (1986) *Biochemistry 25*, 5987–5991.
Pabo, C. O., Sauer, R. T., Sturtevant, J., & Ptashne, M. (1979) *Proc. Natl. Acad. Sci. U.S.A. 76*, 1608–1612.
Sauer, R. T., & Anderegg, R. (1978) *Biochemistry 17*, 1092–1100.
Sauer, R. T., Pabo, C. O., Meyer, B. J., Ptashne, M., & Backman, K. C. (1979) *Nature (London) 279*, 396–400.
Sauer, R. T., Hehir, K., Stearman, R. S., Weiss, M. A., Jeitler-Nilsson, A., Suchanek, E. G., & Pabo, C. O. (1986) *Biochemistry 25*, 5992–5998.
States, D. J., Haberkorn, R. A., & Ruben, D. J. (1982) *J. Magn. Reson. 48*, 286–292.
States, D. J., Dobson, C. M., Karplus, M., & Creighton, T. E. (1984) *J. Mol. Biol. 174*, 411–418.
Thomas, G. J., Jr., Prescott, B., Benevides, J. M., & Weiss, M. A. (1986) *Biochemistry 25*, 6768–6778.
Weiss, M. A., Sauer, R. T., Patel, D. J., & Karplus, M. (1984) *Biochemistry 23*, 5090–5095.
Weiss, M. A., Stearman, R., Jeitler-Nilsson, A., Karplus, M., & Sauer, R. T. (1986) *Biophys. J. 49*, 29–33.
Weiss, M. A., Karplus, M., & Sauer, R. T. (1987) *Biochemistry* (preceding paper in this issue).

Proton Nuclear Magnetic Resonance Studies on Bulge-Containing DNA Oligonucleotides from a Mutational Hot-Spot Sequence†

Sarah A. Woodson and Donald M. Crothers*
Department of Chemistry, Yale University, New Haven, Connecticut 06511
Received June 16, 1986; Revised Manuscript Received September 23, 1986

ABSTRACT: A series of bulge-containing and normal double-helical synthetic oligodeoxyribonucleotides, of sequence corresponding to a frame-shift mutational hot spot in the λ C_I gene, are compared by proton magnetic resonance spectroscopy at 500 MHz. The imino proton resonances of d(GATGGGCAG)·d(CTGCCCATC), d(GATGGGCAG)·d(CTGCCCCATC), and d(GATGGGCAG)·d(CTGACCCATC) are assigned by one-dimensional nuclear Overhauser effect spectroscopy. Nonselective T_1 inversion–recovery experiments are used to determine exchangeable proton lifetimes and to compare helix stability and dynamics of the three duplexes. An extra adenosine flanking the internal G·C base pairs has a strongly localized effect on helix stability, but the destabilizing effect of an extra cytidine in a C tract is delocalized over the entire G·C run. These data lead to the conclusion that the position of the bulge migrates along the run in the fast-exchange limit on the NMR time scale. Rapid migration of the bulge defect in homopolymeric sequences may help rationalize both frame-shift mutagenesis and translational frame shifting. We estimate that the unfavorable free energy of a localized bulge defect is 2.9–3.2 kcal/mol, in good agreement with earlier estimates for RNA helices.

Frame-shift mutations are known to occur predominantly in monotonous runs of base pairs, which can slip one or two positions and still maintain base pairing (Okada et al., 1972; Ames et al., 1973), but the precise role of local DNA structure in mutational events is not yet well understood. Early studies (Lerman, 1963, 1964; Drake, 1964) of mutation genetics led Streisinger to propose a bulged base model for frame-shift

†Supported by Grant GM21966 from the National Institutes of Health.

0006-2960/87/0426-0904$01.50/0